Soft Multi-point Waveguide Sensor for Proprioception and Extereoception in Inflatable Fingers

Ahmed Hassan
Queen Mary University of London,
London, UK
ahmed.hassan@qmul.ac.uk

Faisal Aljaber
Queen Mary University of London,
London, UK
f.aljaber@qmul.ac.uk

Hareesh Godaba
University of Sussex, Brighton
East Sussex, UK
hg322@sussex.ac.uk

Ivan Vitanov
Queen Mary University of London,
London, UK
i.vitanov@qmul.ac.uk

Kaspar Althoefer
Queen Mary University of London,
London, UK
k.althoefer@qmul.ac.uk

***Abstract*—Disadvantages of conventional robotic systems include rigidity, multiple moving parts, and the need for elaborate safety mechanisms when used in human-machine interaction. Soft manipulators and grippers are gaining in popularity due to being able to handle large payloads whilst being lightweight, highly compliant, low-cost, and compactible or collapsible. Yet soft robots cannot make use of traditional rigid sensors to measure their pose or interaction with the environment. Perception in soft robotics needs to embrace alternative methods: sensors made from soft materials that perform robustly under compression and bending conditions; i.e, stretchable soft sensors that rely on (their) material and electrical properties to output signal measurements. However, many such sensors come with inherent drawbacks, including material incompatibility, fabrication complexity, and hysteresis. In this paper, we report on the use of multiple staggered optical waveguide sensors embedded in silicone. These stretchable optical waveguide sensors coated with a thin layer of gold were fabricated and integrated with a fabric-based, inflatable robot finger. An experimental study was performed to evaluate the sensor's responsiveness. We find that multi-curvature pose estimation (from 0.05-0.135 m^{-}1) (from fully deflated to maximum inflation) can be acquired after integration with the inflatable robot finger. The sensor proves capable of measuring force information by way of interaction with the environment at multiple points along the gripper.**

***Index Terms*—Soft fabric finger, optical-based sensing, soft sensor**

I. Introduction

Soft robots are growing in prominence due to the associated safety, compliance, low cost and simple control needed to operate them [1],[2]. Fabric-based soft robots are particularly promising due to a number of unique, innate attributes, including being lightweight and collapsible. Fabric-based actuators are also very low cost and can be manufactured in bulk, via industrial or programmed sewing machines, to generate complex shapes [3]. As such, various soft robotic devices have been developed using fabric-based structures, yielding high payload capacity manipulators [4], [5], soft grippers [6], and rehabilitation gloves [7], [8].

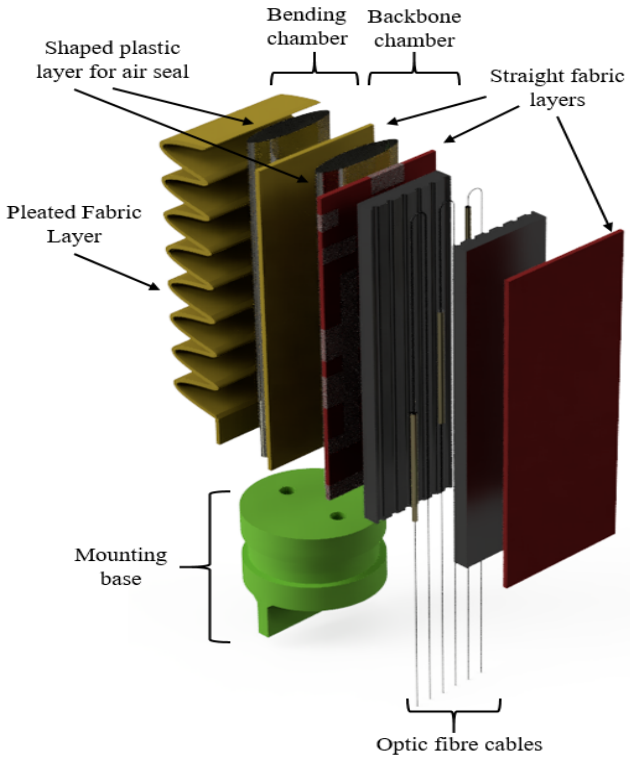

Fig. 1. Exploded view for soft fabric-based pneumatic actuator (SFPA) assembly showing actuator structure and optic fibre cables connected to waveguides.

The challenge lies in developing soft sensors to enable proprioception of soft fabric actuators without compromising their natural advantages. Fabric-based robot arms and fingers are predominantly cylindrical structures with folds and

pleated structures integrated to achieve bending. Cappello et al. showed how different layering arrangements of fabrics in a pleated geometry can give rise to a range of multi-degree-of-freedom actuators that can operate at low pressures, have a high torque-to-weight ratio and are fully collapsible [7]. Although they present interesting attributes, such actuators pose major challenges concerning sensorisation and proprioception. Firstly, the outer regions are generally made up of features such as pleats or folds, which are not ideal for integrating sensor elements. Secondly, fabrics are more pliable as compared to pneumatic actuators and hence exhibit high local curvatures which are difficult to measure with integrated sensors. One practical solution is to embed pure bending sensors along the inextensible fabric layer. Elgeneidy et al. embedded commercially available flex sensors into the strain limiting layer of a soft pneumatic finger to characterise bending [9].

Recent studies have shown that stretchable optical waveguides made of transparent elastomeric materials can be utilised to sense longitudinal elongation and bending. Zhao et al. developed stretchable waveguides and integrated them in a soft pneumatic hand to sense bending and normal forces applied to the hand [10]. Teeple et al. used similar sensors in a pneumatic gripper and showed that they are robust to environmental conditions and can be used for deep-sea grasping and manipulation [11]. Stretchable waveguides and optical deflections in an optoelectronic foam have also been used to detect the shape of a soft body, such as bending and twisting as well as direction [12][15]. All these studies have designed optical waveguides that run along the length of the soft bodies but have not addressed local deformations in these bodies. Many studies in the literature, utilising different sensing technologies, also assume constant curvature in the soft actuators to localise the state with strain or flex sensors[13]. However, as the softness of the bodies increases, they are more prone to exhibit inhomogeneous deformations. In particular, fabric-based soft actuators can conform well to the shape of an object and thereby assume shapes that are not homogeneously curved.

Soft optical-based sensors working on the principle of light intensity modulation have exhibited excellent stability, consistency, and ruggedness for applications like deep-sea grasping [16]. Waveguides with highly elastic capability embedded in optoelectronic silicone matrices have also been utilised for the detection of various deformation modes, such as twisting and bending, and can be used for position perception in soft robots (proprioception) [17], [18].

In view of the above, the contributions proposed in this paper are the following: 1) Design and fabrication of a soft fabric-based, inflatable finger with easy sensor integration for bending measurement. 2) Creation and design of a soft optical multi-point waveguide sensor for proprioception and extereoception in soft fabric-based, inflatable fingers.

II. Materials and Methods

The proposed sensor consists of two main parts: 1) the sensing elements which are the stretchable optical waveguides and 2) the housing as per Fig. 2(a).

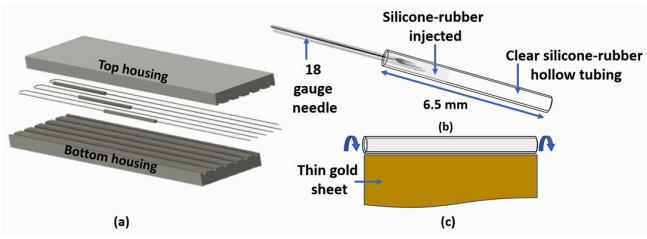

Fig. 2. a) Schematic of the sensor and its different components b) The process of injecting the silicone-gel into the flexible silicone tubing c) The process of applying the thin gold layer

A. Fabrication of the stretchable optical waveguides

Polydimethylsiloxane (PDMS) is one of the most common polymeric materials employed for optical sensing applications due to its inherent compatibility with optical fibres and transparency. Nevertheless, typical PDMS used are known for their relatively low elongation at break, which indicates lower stretchability [18]. Even though there is a considerable range of commercially available highly stretchable elastomers, barely any of them are optically transparent and compatible with other sensing modalities. For our waveguide fabrication, we have utilised a hybrid of different materials consisting of off-the-shelf clear flexible silicone rubber tubes with refractive index between 1.35 and 1.4 and a transparent silicone gel (Solaris™, Smooth-On) which has a high refractive index of 1.41, elongation of 290% at break, and a tensile strength of 1.24 KPa. A single waveguide is created by preparing the silicone gel mixture through mixing the two materials A and B of Solaris™, Smooth-On in a ratio of 1:1, and then carefully pouring the mixture into a syringe. An 18 gauge needle head is used to inject the transparent silicone gel mixture into the clear flexible silicone rubber tube to create the waveguide, as shown in Fig. 2(b). The silicone is then left to cure for 24 hours at room temperature (here: 23°C). The resultant waveguide is a cylindrical structure whose core and outer diameters are 1 mm and 2 mm, respectively, as shown in Fig. 3(a). The encapsulation of the transparent silicone gel mixture in a clear flexible silicone rubber tube preserves the cylindrical shape of the waveguide and makes waveguide integration and handling easier. Commercially available flexible optical fibres (Super Eska™ Simple Fibre Cable SH100-01) of inner and outer diameters of 0.25 mm and 1 mm, respectively, are then segmented and connected to both ends of the waveguide and secured using Loctite super-glue. Connecting the optical fibres to both ends of the waveguide makes it more sensitive and responsive to mechanical deformation (compression and bending) compared to other configurations using strapped optical fibres. It further removes the limitation of the bending radius of the optical fibers, as specified by the manufacturer. The

extrinsic property (outer reflective layer) of the waveguides is modified by adding a thin gold-coated layer on the outside. The gold layer is attached to the waveguide using a special gold gluing liquid provided by Winsor Newton, see Fig. 2(c). The thin gold layer is added to improve the waveguide's response and for light intensity modulation (LIM).

The design and fabrication approaches implemented in this study were intended to be simple, cost-effective, and less time-consuming. To fabricate the waveguide and to apply the thin gold leaf, the process was kept simple compared to the process presented in [24], in which sputter deposition was used to apply the gold reflective layer – this process is expensive and uniform distribution is not always guaranteed. The soft sensor contains three small-size waveguides in one soft-structured block, unlike the relatively large-sized waveguides fabricated in both studies [25],[26], which use bulky components. This makes our sensor easy to integrate into the finger, by sliding the sensor easily inside a fold created specially to hold the sensor; as opposed to the embedded optical fibre-based design approach in [27], which in the event of any permanent damage to the sensor might compromise the whole design, and with it, the performance of the articulated structure.

B. Fabrication of Sensor Housing Elements

In the final design of the sensor housing, a four-step process was followed. First, two separate rectangular moulds were designed using CAD software (AUTODESK, Fusion 360). Then the moulds were fabricated using a commercial Ultimaker 3 Dual Extruder 3D printer with low-cost PLA (polylactic acid), as Fig. 3(a) shows. To allow the three pairs of optical fibres (each pair consists of a transmitting fibre and a receiving fibre) to join with the optical waveguides within the soft housing, they are placed inside the bottom mould and fed through 2 mm diameter apertures at either end of the mould, as shown in Fig. 3(a). Significantly, the optical waveguides are placed and secured within the bottom mould in a staggered configuration with an offset of 4 cm between each pair of waveguides; self-adhesive measuring tape was used to ensure consistent offset between the three waveguides (see Fig. 3a). The housing has a depth, length, and width of 1.3 cm, 16.6 cm, and 4 cm, respectively. Each waveguide has a length of 6.5 cm. The top mould was connected to the bottom mould by strong tape to prevent any leakage during the process of injecting the silicone. Finally, the soft housing layers were made by pouring a pre-cured mixture of A and B in a ratio of 1:1 of DragonSkin 30 into the mould to form the final sensor structure shown in Fig. 3(b). Black colour was added to prevent light beams from being scattered laterally between waveguides.

C. Soft Inflatable Finger Fabrication

The fabric-based, inflatable finger used in this study is made from airtight fabric, Ripstop. It is formed by a three-layer/dual-chamber inflatable structure, extending previous work [21]. An exploded view detailing the construction of the fabric-based finger is shown in Fig. 1. Be it noted that in our design the structure can be thought of as both finger and

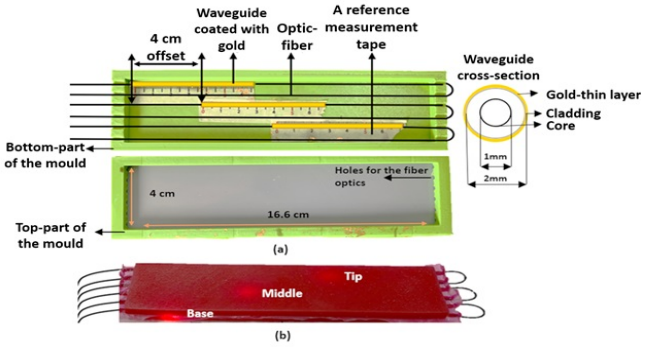

Fig. 3. (a) Waveguide placement inside the 3D printed mold with a 4cm offset. Optic fibres are inserted through the 6 apertures made at each end of the mould. The cross-section of a single waveguide is shown revealing each layer of the waveguide (b) Light transmitted through the three integrated waveguides at the base, in the center, and at the tip of the sensor structure.

actuator simultaneously. For constructing the actuator, pre-shaped fabric sheets are folded in layers to create the required folds or pleats. The fabrication process involves joining pre-cut pieces of fabric folded in layers to create the required pleats by sewing. The fabric sheet is then sewn along its edges to keep the folds in place. The sheet with the integrated folds is then sewn onto the fabric sheet that will form the middle sheet. The fused sheets are folded back again, and a third fabric sheet is sewn onto a previously prepared pair of fabric sheets. The two chambers of the SFG are each connected to two separate tubes for individual air supply. Making the fabric structure airtight is accomplished by adding a membrane made of plastic sheeting. The plastic sheets are formed into the desired shape using a heat sealer. The length of the plastic sheet for the bending chamber (Chamber 1) is greater than that of the backbone chamber (Chamber 2) to allow for unrestricted bending of the gripper. A third chamber of 8 cm width is added to allow easy coupling of the sensor and the finger, as Fig. 1 shows. The finger has a total length of 22 cm, with 7 pleats in the bending chamber of 2.5 cm each. For integrating the sensor structure proposed in this paper, an extra chamber is created by sewing on another fabric layer, as shown in Fig. 1.

III. Experimental Protocols and Setup

A. Staggered Soft Optical Waveguide Sensor

Our soft sensor contains three stretchable waveguides, with an offset of 4 cm between them, to allow acquisition of sensory information at multiple points (here: 3) along the sensor's length. Two experiments were performed on the created sensor prototype. First, a compression test using an Instron 5967 Universal Testing Machine (UTM) was carried out. The purpose was to investigate the sensor's signal response, sensitivity, and consistency of output signals for each waveguide when compressed. The UTM is loaded with a 30 kN loading cell, and it was programmed to apply 6 compression cycles of 3 mm depth in total at a speed of 0.5mm/s, interrupted after holding the position for 10 seconds at each compression step.

The second experiment is a bending test. The bending test includes recording the sensor's signal outputs when no bending is applied, then wrapping it around three cylinders with different diameters, ranging from 5 to 7 to 11 cm. All signals are read by a NI USB DAQ 6003 unit (Data Acquisition Card, National Instruments) and saved to an Excel sheet.

B. Soft Inflatable Finger

The bending response of the finger was tested by connecting the pressure controlling unit to a voltage-controlled power supply, where the voltage of the power supply is proportional to the pressure output to the finger. The voltage of the power supply is increased by 0.01 V between 0.03 V and 0.14, with 5 seconds delay between each increment. SFG images for different bending poses were captured using a camera (to serve as ground truth) and processed, and their corresponding pressure values were recorded.

The experiment involving the inflatable finger integrated with the staggered optical waveguides was conducted in similar fashion, with the delay time modified to 10 seconds. These two bending experiments aim to study the performance of both the actuator and the sensor, as well as the effect of the sensor weight on the finger's bending performance.

IV. Results

A. Staggered Soft Optical Waveguide Sensor

1) Compression response test*:* Various optical sensing techniques exist for soft bodies, specifically, for pressure sensing [19], [22]. For our sensor, the modulation method adopted is similar to the method reported in [14], [18], and [23]. Upon deformation of the sensor structure, the micro-cracks formed by the gold coating allow the light to escape and the light intensity can be modulated for the deformation. The sensors based on waveguides are known to be very sensitive to any mechanical deformation applied to them given their soft inherent nature.

The sensor is placed on the UTM flat plate and connected to the measurement system for data acquisition. Fig. 4(a) to Fig. 4(c) shows the response of the sensor on those locations where the waveguides are placed within the sensor structure as Fig. Fig. 3(b) shows. The responses of the different waveguides in Fig. 4(a) to Fig. 4(c) shows the sensitivity of the waveguides when mechanical compression is applied by the UTM with a slow speed rate of 0.5 mm/s with a maximum compression depth of 3 mm along the entire length of the 16.6 cm long sensor. The outputs of the sensor's waveguides increase as the compression force increases from 0 N to 30 N in 5 N increments, in Fig. 4(a) to Fig. 4(c). This proportional increase of the compression is done from 0 mm to 3 mm in an incremental speed rate of 0.5 mm/sec. The compression force and depth have an inverse effect on the output of the waveguides, which means as the force increases gradually on the waveguides, the voltage output of the waveguides decreases as shown in Fig. 4. This behaviour continues until the output voltage reaches the lowest point which is between 0.3 and 0.4 V/V0. The signal (V/V0) which is the voltage recorded through time divided by the highest initial voltage. All responses seem to have a consistent output corresponding to the force applied and they appear to be very sensitive and responsive to the compression force.

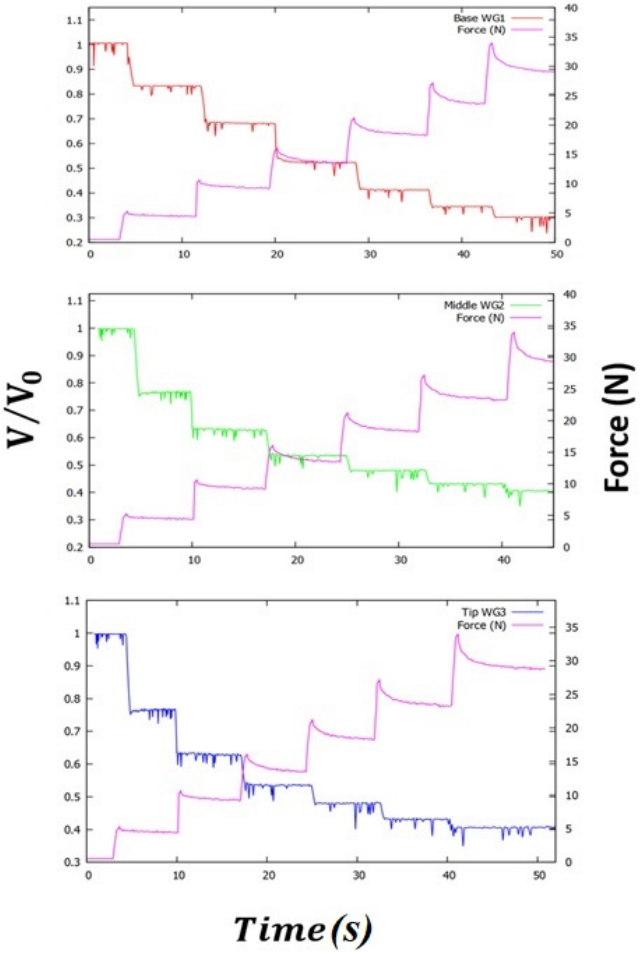

Fig. 4. The compression response of the three waveguides in the staggered sensor a) The base waveguide response against the force applied b) The middle waveguide response c) The tip waveguide.

B. Soft Inflatable Finger

1) Bending response test*:* The staggered waveguide sensor bending test is performed by bending the sensor around three different cylindrical rings that range in diameter from 11 cm to 5 cm. Fig. 6 shows the (V/V0) output signal against the curvature. The response of each waveguide is shown from a resting state through to the point of bending around the smallest circle of 5 cm. As the curvature increases the sensor output gradually decreases, reaching the lowest point of signal registration between 0.3 and 0.2. All waveguides exhibit similar behaviour, i.e. as the bending curvature increases, the waveguide responses decrease, as shown in Fig. 6. From Fig. 6 we can see that the waveguide in the middle is the most affected by the bending out of the three waveguides because

of its location, i.e. the site where maximal bending occurs because of the curvature.

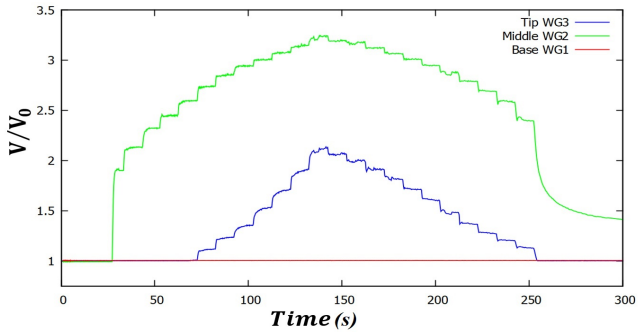

Fig. 5. Output voltage versus time graph for the real-time bending behaviour of the soft fabric-based finger. The bending was achieved by applying increasing values of input air pressure, from 0 kPa to a maximum pressure value of 27.3 kPa and then back to 0 kPa.

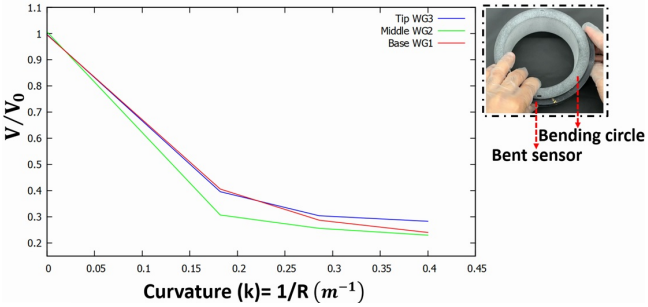

Fig. 6. The response of each waveguide of the sensor when bent around three different rings of diameter 11 cm, 7 cm, and 5 cm to form various curvatures.

C. Sensorisation of the Soft Inflatable Finger

The soft fabric-based finger is tested first without the sensor to record the curvature response through the bending process due to pressure. The images in Fig. 7 show various curvatures captured in real time. The values of actuation pressure used were 0 kPa, 7.34 kPa, 10.48 kPa, 14.17 kPa, 17.96 kPa and 21.37 kPa.

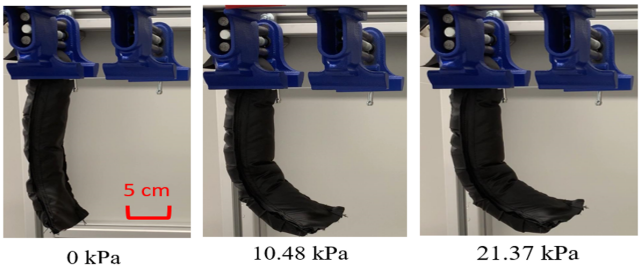

Fig. 7. The bending motion of soft fabric finger under different actuation pressures before the integration of the sensor.

The bending experiment was repeated with the sensor encased in the fabric finger. In this experiment, the finger did not achieve the same curvature under similar input pressure conditions due to the added weight of the sensor. The weight of the sensor is 85 g, which is much greater than that of the finger. Fig. 8 shows snapshots of the sensorised finger as it is bending towards its maximal curvature. The sensor-response-to-curvature plot in Fig. 9 shows the responsiveness and the sensitivity of the sensor to bending pressure. As the curvature increases gradually, the sensor output falls off gently, exhibiting a gradual and stable decrease in signal magnitude until reaching the point of saturation, when the sensor is no longer responsive.

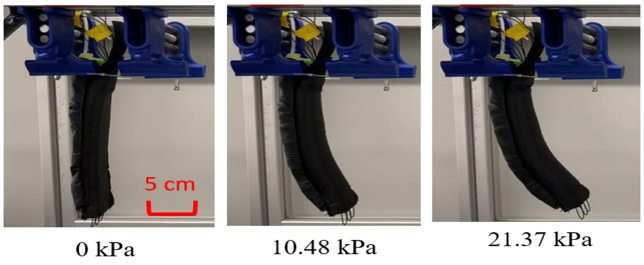

Fig. 8. Soft fabric-based gripper with integrated optical waveguide sensor bending under different pressure values. The sensor registers deformations due to bending movements at 3 points along the actuator.

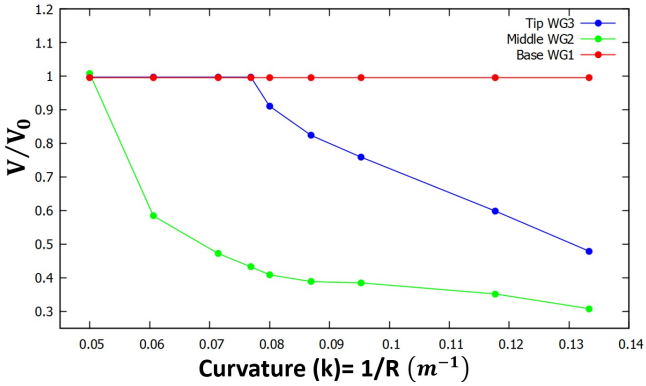

Fig. 9. Soft fabric-based finger with integrated optical waveguide sensor bending under different pressure values. The sensor registers deformations due to bending movements at 3 points along the actuator.

As evident from Fig. 9, most of the bending in the fabric gripper takes place at the middle point (the green signal) of the finger. That is why, as soon as the pressure increases, we see the change in the V/Vo output of the middle waveguide. After some time, the signal from the tip waveguide (the blue signal) starts to change, signalling onset of the bending effect at the tip of the finger. An interesting point to note is that the output from the base waveguide (the red signal) is completely unaffected during the whole bending operation showing that the bending effect is essentially absent at the base. So we can see that the proposed sensor has been successful in recording the movement at various points along the finger.

By comparing the pressure vs curvature responses of the fabric finger with sensor integration (black line) and without sensor integration (orange line) in Fig. 10 shows that integrating the sensor with the fabric finger significantly limits the

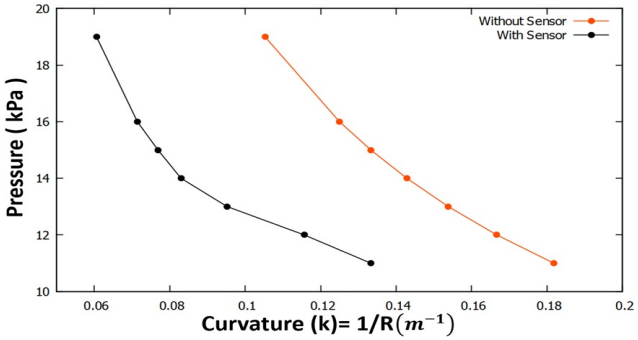

Fig. 10. The bending curvature versus the input pressure plots for the fabric finger both with and without sensor integration. It is observed that adding the sensor significantly reduces the bending capability of the fabric gripper under the same input pressure conditions.

maximum curvature available to the fabric-based finger. This is because the fabric-based finger weighs much less than the sensor block and greater amount of force is required to achieve the same amount of curvature with sensor integration than without. Also, the integration of the sensor block increases the stiffness of the finger, which needs to be overcome through increased actuation pressure.

V. Conclusions and Future Work

In this study, we report on the novel design and fabrication of both a staggered soft optical waveguide sensor and a soft fabric-based finger. The sensor was found to be sensitive and responsive during both mechanical compression and bending tests. The output of the sensor's waveguides is found to be location-dependent. The soft finger, absent the sensor, is more flexible and able to bend more versus when it is integrated with the sensor block, due to the added weight and motion obstruction.

Future work is planned on a new and improved sensor design of lower size and weight utilising micro-waveguides. The finger can also be improved to ensure smoother bending. An algorithm to reconstruct the shape of the finger modelled as a backbone curve would enable kinematic analysis to be performed with a view to calibration and (model-based) control.

References

[1] D. Rus and M. T. Tolley, "Design, fabrication and control of soft robots," Nature, vol. 521, no. 7553, pp. 467–475, May 2015.

[2] M. Cianchetti, T. Ranzani, G. Gerboni, T. Nanayakkara, K. Althoefer, P. Dasgupta, and A. Menciassi, "Soft robotics technologies to address shortcomings in today's minimally invasive surgery: the STIFF-FLOP approach," Soft Robot., vol. 1, no. 2, pp. 122–131, 2014.

[3] L. Cappello, K. C. Galloway, S. Sanan, D. A. Wagner, R. Granberry, S. Engelhardt, F. L. Haufe, J. D. Peisner, and C. J. Walsh, "Exploiting textile mechanical anisotropy for fabric-based pneumatic actuators," Soft Robot., vol. 5, no. 5, pp. 662–674, 2018.

[4] X. Liang, H. Cheong, Y. Sun, J. Guo, C. K. Chui, and C.-H. Yeow, "Design, Characterization, and Implementation of a Two-DOF Fabric-Based Soft Robotic Arm," IEEE Robot. Autom. Lett., vol. 3, no. 3, pp. 2702–2709, 2018.

[5] X. Liang, H. Cheong, C. K. Chui, and C.-H. Yeow, "A Fabric-Based Wearable Soft Robotic Limb," J. Mech. Robot., vol. 11, no. 3, p. 31003, 2019.

[6] A. Hassan, H. Godaba, and K. Althoefer, "Design Analysis of a Fabric Based Lightweight Robotic Gripper," in Annual Conference Towards Autonomous Robotic Systems, 2019, pp. 16–27.

[7] L. Cappello, J. T. Meyer, K. C. Galloway, J. D. Peisner, R. Granberry, D. A. Wagner, S. Engelhardt, S. Paganoni, and C. J. Walsh, "Assisting hand function after spinal cord injury with a fabric-based soft robotic glove," J. Neuroeng. Rehabil., vol. 15, no. 1, p. 59, 2018.

[8] H. K. Yap, P. M. Khin, T. H. Koh, Y. Sun, X. Liang, J. H. Lim, and C.-H. Yeow, "A fully fabric-based bidirectional soft robotic glove for assistance and rehabilitation of hand impaired patients," IEEE Robot. Autom. Lett., vol. 2, no. 3, pp. 1383–1390, 2017.

[9] K. Elgeneidy, N. Lohse, and M. Jackson, "Bending angle prediction and control of soft pneumatic actuators with embedded flex sensors–a data-driven approach," Mechatronics, vol. 50, pp. 234–247, 2018.

[10] H. Zhao, K. O'Brien, S. Li, and R. F. Shepherd, "Optoelectronically innervated soft prosthetic hand via stretchable optical waveguides," Sci. Robot., vol. 1, no. 1, p. eaai7529, 2016.

[11] C. B. Teeple, K. P. Becker, and R. J. Wood, "Soft curvature and contact force sensors for deep-sea grasping via soft optical waveguides," in 2018 IEEE/RSJ International Conference on Intelligent Robots and Systems (IROS), 2018, pp. 1621–1627.

[12] I. M. Van Meerbeek, C. M. De Sa, and R. F. Shepherd, "Soft optoelectronic sensory foams with proprioception," Sci. Robot., vol. 3, no. 24, p. eaau2489, 2018.

[13] T. C. Searle, K. Althoefer, L. Seneviratne, and H. Liu, "An optical curvature sensor for flexible manipulators," in 2013 IEEE International Conference on Robotics and Automation, 2013, pp. 4415–4420.

[14] G. P. Agrawal, Fiber-optic communication systems, vol. 222. John Wiley Sons, 2012.

[15] Xie, H., Liu, H., Luo, S., Seneviratne, L. D., Althoefer, K. "Fiber optics tactile array probe for tissue palpation during minimally invasive surgery." in 2013 IEEE/RSJ International Conference on Intelligent Robots and Systems (IROS), 2013, pp. 2539-2544.

[16] C. B. Teeple, K. P. Becker, and R. J. Wood, "Soft Curvature and Contact Force Sensors for Deep-Sea Grasping via Soft Optical Waveguides," IEEE Int. Conf. Intell. Robot. Syst., pp. 1621–1627, 2018, doi: 10.1109/IROS.2018.8594270.

[17] I. M. Van Meerbeek, C. M. De Sa, and R. F. Shepherd, "Soft optoelectronic sensory foams with proprioception," Sci. Robot., vol. 3, no. 24, pp. 1–8, 2018, doi: 10.1126/SCIROBOTICS.AAU2489.

[18] K. C. Galloway, Y. Chen, E. Templeton, B. Rife, I. S. Godage, and E. J. Barth, "Fiber Optic Shape Sensing for Soft Robotics," Soft Robot., vol. 6, no. 5, pp. 671–684, 2019, doi: 10.1089/soro.2018.0131.

[19] M. Ramuz, B. C. K. Tee, J. B. H. Tok, and Z. Bao, "Transparent, optical, pressure-sensitive artificial skin for large-area stretchable electronics," Adv. Mater., vol. 24, no. 24, pp. 3223–3227, 2012, doi: 10.1002/adma.201200523.

[20] J. S. Kee, D. P. Poenar, P. Neuzil, and L. Yobas, "Monolithic integration of poly(dimethylsiloxane) waveguides and microfluidics for on-chip absorbance measurements," Sensors Actuators, B Chem., vol. 134, no. 2, pp. 532–538, 2008, doi: 10.1016/j.snb.2008.05.040.

[21] A. Hassan, H. Godaba, and K. Althoefer, Design Analysis of a Fabric Based Lightweight Robotic Gripper, vol. 11649 LNAI. 2019

[22] G. Kodl, "A new optical waveguide pressure sensor using evanescent field," Proc. - Electron. Components Technol. Conf., vol. 2, pp. 1943–1946, 2004, doi: 10.1109/ectc.2004.1320392.

[23] F. Aljaber and K. Althoefer, "Light Intensity-Modulated Bending Sensor Fabrication and Performance Test for Shape Sensing", vol. 11649 LNAI. Springer International Publishing, 2019.

[24] C. To, T. Hellebrekers, J. Jung, S. J. Yoon and Y. Park, "A Soft Optical Waveguide Coupled With Fiber Optics for Dynamic Pressure and Strain Sensing," in IEEE Robotics and Automation Letters, vol. 3, no. 4, pp. 3821-3827, Oct. 2018, doi: 10.1109/LRA.2018.2856937.

[25] Felt, W., Telleria, M.J., Allen, T.F. et al., "An inductance-based sensing system for bellows-driven continuum joints in soft robots", Autonomous Robot 43, 435–448 (2019). https://doi.org/10.1007/s10514-018-9769-7.

[26] H. Zhao, K. O'Brien, S. Li and R. Shepherd, "Optoelectronically innervated soft prosthetic hand via stretchable optical waveguides", in Science Robotics, Issue 1, Dec. 2016, vol. 1, doi: 10.1126/scirobotics.aai7529.

[27] H. Zhao, J. Jalving, R. Huang, R. Knepper, A. Ruina and R. Shepherd, "A Helping Hand: Soft Orthosis with Integrated Optical Strain Sensors and EMG Control," in IEEE Robotics Automation Magazine, vol. 23, no. 3, pp. 55-64, Sept. 2016, doi: 10.1109/MRA.2016.2582216.